Journal of Earth Science, *Vol. 23*, *No. 1*, *p. 88–96*, *February 2012* *ISSN 1674-487X*
Printed in China
DOI: 10.1007/s12583-012-0235-8

TSR-Derived Authigenic Calcites in Triassic Dolomite, NE Sichuan Basin, China—A Case Study of Well HB-1 and Well L-2

Sijing Huang* (黄思静), **Keke Huang** (黄可可)
State Key Laboratory of Oil/Gas Reservoir Geology and Exploitation, *Chengdu University of Technology*, *Chengdu* 610059, *China*; *Institute of Sedimentary Geology*, *Chengdu University of Technology*, *Chengdu* 610059, *China*
Zhiming Li (李志明), **Ming Fan** (范明), **Ershe Xu** (徐二社)
Wuxi Research Institute of Petroleum Geology, *SINOPEC*, *Wuxi* 214151, *China*
Jie Lü (吕杰)
State Key Laboratory of Oil/Gas Reservoir Geology and Exploitation, *Chengdu University of Technology*, *Chengdu* 610059, *China*; *Institute of Sedimentary Geology*, *Chengdu University of Technology*, *Chengdu* 610059, *China*

ABSTRACT: It has been proven that thermochemical sulfate reduction (TSR) took place extensively in the Lower Triassic carbonate reservoirs in Northeast (NE) Sichuan (四川) basin. We have carried out analyses on bulk rock compositions and isotope ratios together with petrography and fluid inclusions to assess the impact of TSR on diagenetic process of Triassic dolomites. In this article, TSR-related burial diagenesis is characterized by precipitation of calcite cement with negative $\delta^{13}C$ values and high homogenization temperature. The light carbon isotopic compositions of this phase indicate that carbon incorporated in this cement was partly derived from oxidation of hydrocarbon. The high homogenization temperatures indicate that the thermochemical reduction of sulfates has been taking place in the deep part of NE Sichuan basin. Additional evidence supporting this interpretation is the high Sr values of this calcite cement. Moreover, the calcites have a $\delta^{18}O$ of -8.51‰ to -2.79‰ PDB and are interpreted to have precipitated from high salinity fluids with $\delta^{18}O$ of +5‰ to +13‰ SMOW. Under cathodoluminescence, these calcite cements appear dark brown or black, and both Mg concentrations and Mn/Sr ratios are low. It is therefore indicated that seawater was the principal agent of precipitation fluids. Finally, it should be noted that although H_2S and CO_2 increased as TSR continued, porosity has been ultimately destroyed by calcite cementation.

KEY WORDS: NE Sichuan basin, Triassic, TSR, calcite cementation, reservoir quality.

INTRODUCTION

Thermochemical sulfate reduction (TSR) has been known as a common and widespread process in Triassic carbonate reservoirs, NE Sichuan basin. The reservoir quality of these marine strata must have been altered by the chemical processes related to TSR, such

This study was supported by the National Natural Science Foundation of China (Nos. 40839908 and 41172099).
*Corresponding author: sjhuang@cdut.edu.cn

Manuscript received October 17, 2010.
Manuscript accepted December 20, 2010.

as hydrocarbon consumption and H_2S and CO_2 generation (Huang et al., 2008a, 2007a, b; Ma et al., 2008, 2007; Wang et al., 2007; Zhu et al., 2006a, b, 2005; Cai et al., 2004). However, although calcite cements must also be produced during TSR, little attention has been given to them. In this article, we will present data from the Feixianguan and Jialingjiang formations on the occurrence, chemical characteristics, and significance of the TSR-originated calcite cements, thus providing a geochemical method that can be used to distinguish the calcite cements produced by TSR.

According to Worden and Smalley (1996), the simplest TSR reaction can be written as

$$CaSO_4+CH_4 \Rightarrow CaCO_3+H_2S+H_2O \quad (1)$$

and the reaction between anhydrite and ethane can be written as

$$2CaSO_4+C_2H_6 \Rightarrow 2CaCO_3+H_2S+S+2H_2O \quad (2)$$

Reactions (1) and (2) provide the most reasonable explanation for both occurrence of authigenic calcite and oxidization of organic matter whose carbon is incorporated into these calcites. According to these two reactions, the so-called TSR-originated calcites must fulfill at least two general criteria.

(1) Low $\delta^{13}C$ values: hydrocarbon is a critical reactant of this process, and oxidation of hydrocarbon usually produces essentially light carbon. Thus, the $\delta^{13}C$ of calcite cements produced by TSR theoretically have very low $\delta^{13}C$ values. Reported $\delta^{13}C$ values of the TSR calcites in Triassic, NE Sichuan basin, range from -10‰ to -20‰ (Huang et al., 2007a; Wang et al., 2007; Zhu et al., 2005). Based on the calculation of Huang (2010), the contribution of organic carbon to TSR calcites ranges from 28% to 52%, and the more the TSR organic carbon source contribution is, the lower the $\delta^{13}C$ values in TSR calcites is.

(2) High precipitation temperature: temperature is the most important factor governing TSR reactions. The lower temperature limit for TSR is suggested to be about 100 to 140 ℃. The fluid-inclusion homogenization temperature from TSR calcites in Triassic, NE Sichuan basin, ranges from 110 to 240 ℃ (Huang et al., 2007a; Wang et al., 2007). The lowest temperature measured was 110 ℃, approximately commensurate with the BSR (bacterial sulfate reduction) upper bound and TSR lower limit as defined by Machel (2001). Most of the measurements are in the range of 130 to 170 ℃ (Wang et al., 2007).

Huang (2010) applied the term "tri-high calcite" to calcite cements in Triassic carbonates, NE Sichuan basin, due to their relatively high negative $\delta^{13}C$ values, high homogenization temperature, and high strontium content.

(3) High Sr contents: Sr contents of calcite cements are interpreted to reflect varied Sr/Ca ratios in the diagenetic fluid. However, the amounts of Sr in sulphate-rich waters should be limited by the relatively low solubility of celestite

$$SO_4^{2-}+Sr^{2+} \Leftrightarrow SrSO_4 \text{ (celestite)} \quad (3)$$

Therefore, to be able to accumulate large amounts of Sr, it is essential that the fluid become depleted in SO_4^{2-}, which may potentially be influenced by TSR. Therefore, before epigenetic celestite precipitated, Sr was extracted from the pore water and fixed in form of calcite cements.

Almost all TSR-derived calcites have the former two features in common. However, high Sr would not be a common feature of all TSR. This is because the presence of Sr-rich cements requires the source of strontium in strata, which is presumably originally composed of aragonite, in that aragonite usually contains very high Sr values. In many Triassic carbonates samples of NE Sichuan basin, it is common to find carbonate grains composed entirely of ooids. Ooids are identified as being composed originally of aragonite on the basis of their intra-cortical leaching observed as Huang et al. (2007a) reported. Had these ooids been originally calcitic, they would not have been leached to produce the intra-cortical moldic pores. Therefore, the source for high strontium is available in Triassic carbonates reservoirs, NE Sichuan basin.

Given the recent interest about the link between the TSR and gas reservoirs, the reexamination of TSR-occurred rocks on the East Sichuan basin is extremely important. Although most early works has proposed certain reasons, such as preserved as the product of dedolomitization, to explain the presence of calcite cements, this article presents clear evidence that Triassic dolomite rocks in NE Sichuan contain abundant calcite cements with "tri-high" signature, which expected relative to TSR alone. Thus, we have evaluated the effect of TSR within these gas reservoirs

upon pore volumes during diagenesis.

SAMPLING AND ANALYTICAL TECHNIQUES

Based on the framework of the present project supported by the National Natural Science Foundation of China, Well HB-1 and Well L-2 were selected for the detailed sampling and measurements. These two wells are located in the joint area of Mount Huaying fastigiated fold belt and Mount Daba fold belt, NE Sichuan basin (Fig. 1). Only one sample is collected from Well L-2 at depth 3 285.89 m (Member 2, Feixianguan Formation of Triassic). Other samples are all collected from Well HB-1 at depths ranging from 4 484.21 to 4 490.01 m (Member 2, Jialingjiang Formation of Triassic). The age effect on isotope record could be ignored due to sampling depth interval spanning only 5.8 m.

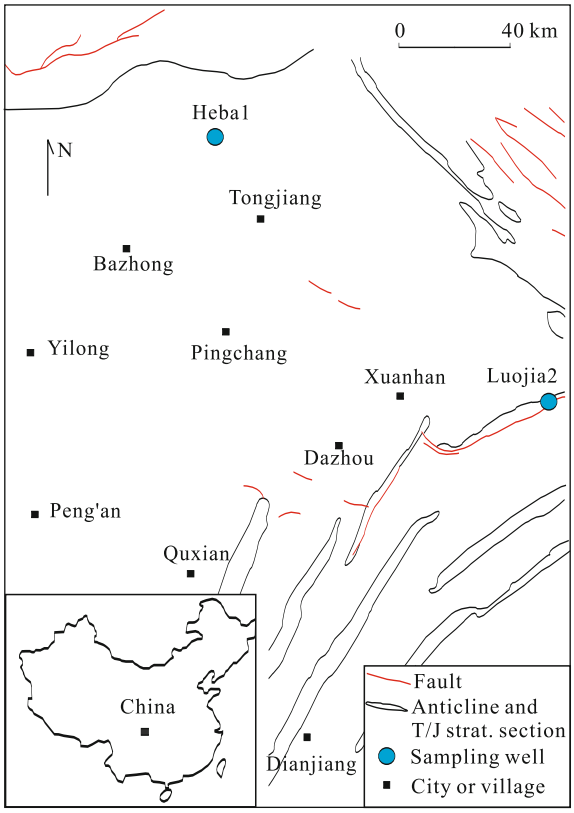

Figure 1. Sketch geological map showing the location of sampling wells.

Petrographic observations were carried out on the uncovered, polished thin sections, some of which were stained by Alizarin Red-S. These thin sections were also prepared for cathodoluminescence (CL) analysis of calcite cements. In thin sections, the mineralogy of the rocks is predominantly calcite and dolomite. Through microscope observation, the predominant mineralogical compositions of the rocks are calcites and dolomites, and calcites occur as blocky calcite spar cements in fill of primary porosity of dolomites.

For chemical analysis, the remaining portions of the samples were crushed into a powder (<200 mesh) and three splits were made for each. One split was preserved for backup, and other two splits were used for element analysis: C and O isotope determinations, respectively. Calcite and dolomite contents of the samples were calculated from the measured CaO and MgO values.

Two major element oxides (CaO and MgO) were analyzed using volumetric analysis method with 0.1% detection limit and 2% error; two trace elements (Mn and Sr) were determined by atomic absorption spectrophotometer with the testing limits of 5×10^{-6} and 42×10^{-6} and 13% and 14% errors, respectively. Fe was analyzed by colorimetry, with the testing limits of 0.01% and the errors less than 8%. These analyses were carried out at the Geological and Mineralogical Testing Center of Huayang in Sichuan. Carbon and oxygen isotope compositions of samples were accomplished at Wuxi Research Institute of Petroleum Geology, Research Institute of Petroleum Exploration and Production, SINOPEC. They were measured in a Finnigan MAT 253 mass spectrometer and reported in the $\delta^{13}C$ and $\delta^{18}O$ notation relative to the PDB standard. SY/T6404-1999 standard was used during the laser fluorination analyses. Precision is on the order of 0.2‰ for $\delta^{13}C$ and $\delta^{18}O$. CL observation was under the Leica microscope using CL8200MK5 luminoscope system. Operating conditions were mean 12 kV and 300 μA.

RESULTS

Thin-section analysis of these calcite cements in the Triassic dolomites revealed two varieties with distinct crystal fabrics (Fig. 2). Some of the cements were composed relatively finely crystalline, developed dispersively in intercrystal pores of silty to finely crystalline dolomite (Figs. 2a–2c). Because such small size place severe constraints on the application of basic geochemical techniques, geochemical information of these calcites have been partially masked by the

dolomite matrix, thus, they were regarded as the products of dedolomitization before. The second variety of cements was composed of much larger crystalline, felted calcite crystals (Fig. 2d), and such relatively large size allows the worker to easily determine their origin. Individual crystals of these dolomites exhibit planar-e (euhedral) to planar-s (subhedral) textures. The absence of both euryhaline and stenohaline organisms, the abundant stromatolite structure, and the present of interbedded gypsum would suggest that the sediments in Member 2 of the Jialingjiang Formation have been dolomitized by hypersaline and high Mg/Ca ratio fluid.

Table 1 provides the bulk-geochemistry data for all silty to finely crystalline dolomite samples. The calcite content varies between 1.26% and 98.83% based on calculation of MgO and CaO values of the chemical analysis. Two samples of extremely low MgO content (calculated calcite >98%, almost the pure secondary calcite) are characterized by extremely low $\delta^{13}C$ values (-20.23‰ and -16.19‰, respectively), very high strontium content (1 564 ppm and 3 400 ppm, respectively), and relatively high homogenization temperatures (one of the samples shown in Fig. 2d has the temperature range of 114–134 ℃; mean T_h is 125 ℃). Their unusual element and isotope composition verifies the interpretation that calcite cements have a TSR origin. In contrast, the calcite content of other 16 samples is relatively low (varies between 1.26% and 17.84%). Their $\delta^{13}C$ values show a moderate scattering in the ranges of 1.57‰ to 7.02‰ and their Sr content drops to the range of 80 ppm to 385 ppm. These two geochemical parameters cannot be used directly as evidence in support of cement formation via TSR, so they will be discussed more fully below.

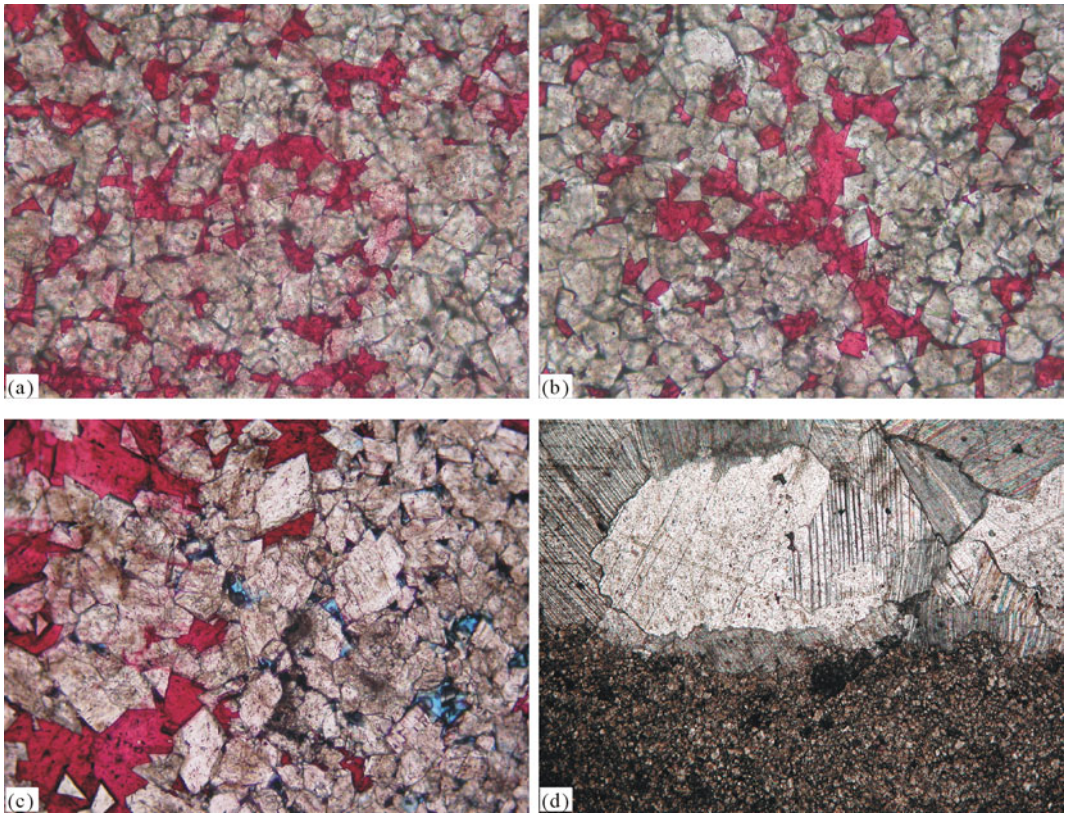

Figure 2. Thin-section photomicrographs showing TSR calcite cements features in finely-silty crystalline dolomites. All images are plane light. (a)–(c) Extensive finely crystalline calcite (stained to discriminate against dolomite) cements fill pore spaces among the dolomite crystals, Well HB-1, Member 2, Jialingjiang Formation; the diagonal line of the image is 0.75 mm; (d) TSR calcite occurs as white, large crystals that grew out from the edge of the dolomite matrix, which is the dark, fine-grained material in the bottom of the image, Well L-2, Member 2, Feixianguan Formation; the diagonal line of the image is 3.75 mm.

Table 1 CaO, MgO, Mn, Sr, Fe, $\delta^{13}C$, and $\delta^{18}O$ statistics and calcite and dolomite contents for Triassic dolomites containing calcite cements of interest

Well	Member	Sample ID	Calcite (%)	Dolomite (%)	Element composition						Isotope composition	
					CaO (%)	MgO (%)	Mn (10^{-6})	Sr (10^{-6})	Mn/Sr	Fe (10^{-6})	$\delta^{13}C$ (‰)	$\delta^{18}O$ (‰)
HB-1	J2	HB-1	14.35	85.85	33.88	18.66	17.31	384.75	0.045	526.68	1.57	-4.04
HB-1	J2	HB-2	11.94	87.29	32.96	18.98	22.25	224.26	0.099	942.49	4.23	-3.90
HB-1	J2	HB-2	4.42	93.54	30.64	20.33	24.45	135.53	0.180	916.12	5.21	-3.70
HB-1	J2	*HB-2	98.83	1.91	55.79	0.41	63.00	1 564.00	0.040	300.00	-20.23	-8.51
HB-1	J2	HB-3	5.19	93.19	30.96	20.26	27.56	156.23	0.176	582.81	5.35	-3.81
HB-1	J2	HB-3	3.92	94.94	30.78	20.64	11.92	140.39	0.085	617.18	5.62	-3.40
HB-1	J2	HB-3	3.57	94.56	30.48	20.56	17.66	126.34	0.140	740.01	5.76	-3.50
HB-1	J2	HB-4	1.63	96.63	30.02	21.01	23.74	97.37	0.244	867.08	5.99	-3.21
HB-1	J2	HB-5	9.48	88.47	31.94	19.23	27.86	193.87	0.144	891.79	5.44	-4.21
HB-1	J2	HB-6	2.10	95.34	29.89	20.73	22.78	95.05	0.240	1 576.12	6.33	-3.31
HB-1	J2	HB-7	8.75	92.07	32.62	20.02	58.47	104.29	0.561	4 486.44	5.72	-4.02
HB-1	J2	HB-7	1.26	94.34	29.12	20.51	29.51	86.56	0.341	2 765.13	6.50	-3.14
HB-1	J2	HB-7	8.75	92.07	32.62	20.02	58.47	104.29	0.561	4 486.62	5.72	-4.02
HB-1	J2	HB-8	17.84	82.83	34.91	18.01	13.11	367.37	0.036	383.26	2.52	-4.36
HB-1	J2	HB-9	2.09	96.20	30.14	20.91	26.09	87.19	0.299	1 449.94	7.02	-2.79
HB-1	J2	HB-10	2.19	94.58	29.71	20.56	27.14	113.58	0.239	2 317.61	6.84	-3.59
HB-1	J2	HB-11	10.70	91.23	33.46	19.83	70.85	154.38	0.459	2 881.53	6.32	-4.16
L-2	F2	*L-1	98.32	0.74	55.15	0.16	15.00	3 400.00	0.004	52.00	-16.19	-7.91

J2 is the Member 2 of Jialingjiang Formation in Triassic; F2 for Member 2 of Feixianguan Formation in Triassic; total sampling interval is 5.8 m; the same sample with different calcite and dolomite contents and correspondingly chemical and isotopic composition has the same sample ID. *. The samples represent almost the pure secondary calcite; see text for detailed discussion.

DISCUSSION

Carbon Isotopic Composition and Carbon Source of Calcite

A global coal gap of Early Triassic has yet confirmed that demise of vascular land plants lasted several million years into Early Triassic (Korte et al., 2003). Such scenario must have resulted in advanced continental weathering that produced widespread clastic successions such as the up to 700 m thick Werfen Group of the Western Carpathians and the Alps (Broglio Loriga et al., 1986), the "Alpine Buntsandstein" in the Northern Alps, the up to 4 000 m thick Buntsandstein of the Germanic basin (Lepper and Röhling, 1998), and the 200 to 600 m thick Moenkopi Formation of western North America (McKee, 1954). Therefore, it is difficult to obtain coeval seawater information, thus, the research on the carbon isotope composition of paleoseawater in this period is insufficient. Investigations of sections in South China (Payne et al., 2004) and Iran (Horacek et al., 2007) have revealed $\delta^{13}C$ curves for Early Triassic, which yield high isotopic values up to around +5‰ and rise to a maximum near +7‰. For these two sections, the samples with high dolomite content do not show any deviation in their carbon isotope ratio with respect to dolomite-poor samples. Hence, the high $\delta^{13}C$ values for seawater of that temporal interval are credible. The $\delta^{13}C$ values of the 16 dolomite samples with low calcite cements (mean=+5.38‰) in our study in general agree with those of their studied and thus primarily reflect inheritance of marine carbon.

For those 17 samples taken from Well HB-1,

their isotopic difference controlled by age could be ignored due to the small sampling interval. It seems that other factors responsible for these isotope variations must be taken into account. In order to clarify this question, the $\delta^{13}C$, $\delta^{18}O$, and Sr contents of these samples are plotted against the amounts of calcite cements (Fig. 3).

Clearly, a definite relationship is visible between the $\delta^{13}C$ values and calcite contents. Figure 3a shows that the negative correlation of them yields a R value of 0.99. In Fig. 3b, the bottommost data point in Fig. 3a, which represents the sample with high calcite content approximately equal to 100%, is excluded and the R value for the linear relationship is 0.89. This result reflects the enrichment of ^{12}C in calcite. On the basis of the correlation between both parameters (using the best-fit line), $\delta^{13}C$ can be formulated as a function of calcite percent: assuming sample with a composition of 100% calcite, the $\delta^{13}C$ value would have been reduced to -20‰ from Fig. 3a and -14‰ from Fig. 3b. According to the calculation of Huang et al. (2010), the relative contribution of organic carbon source for the $\delta^{13}C$ values of -20‰ and -14‰ of authigenic calcites are 57% and 40%, respectively. So, the formation of these calcites is controlled primarily by TSR rather than dedolomitization.

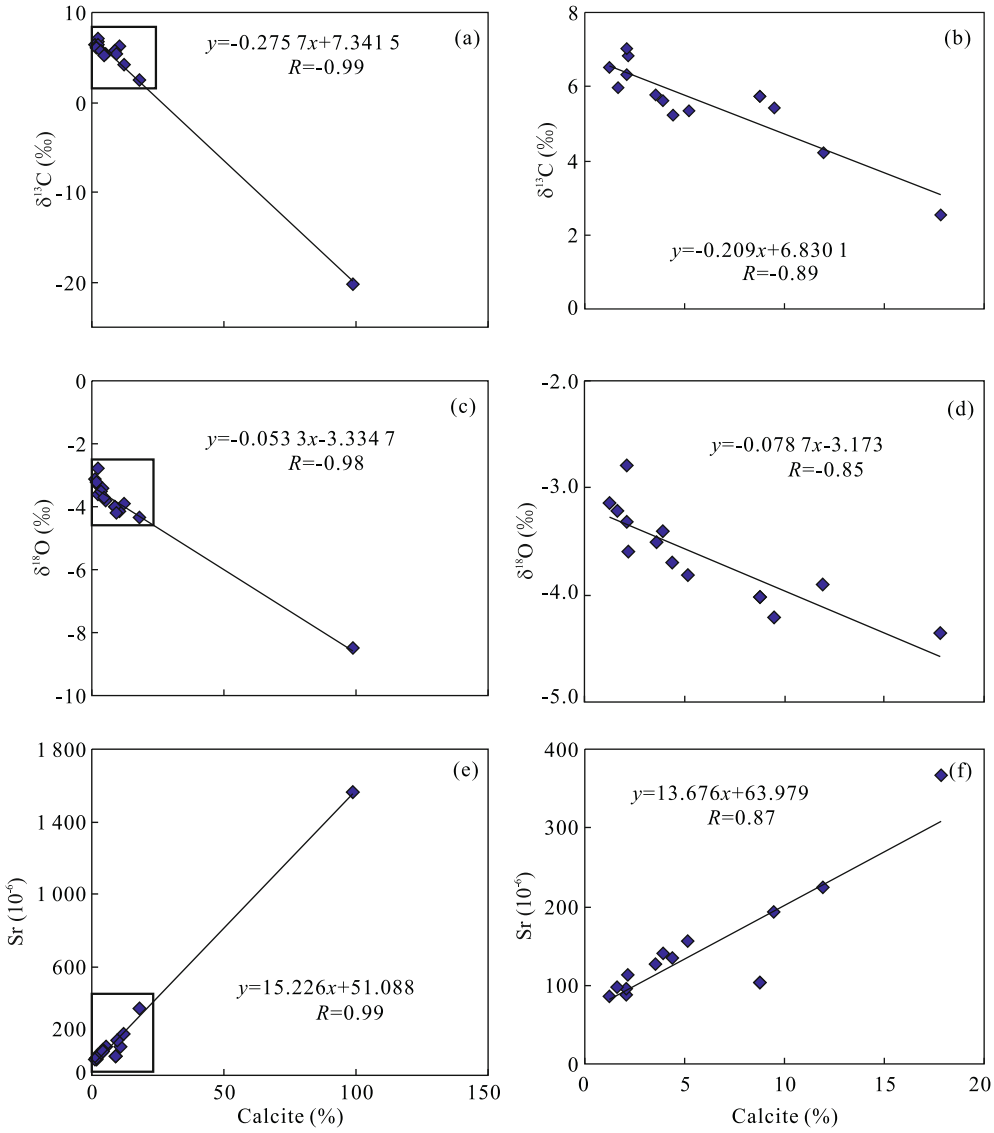

Figure 3. Plots of $\delta^{13}C$, $\delta^{18}O$, and Sr concentration vs. calcite content for the 17 samples sampled from Well HB-1. the depth interval of all samples is 5.8 m; (b), (d), and (f) represent the rectangles of (a), (c), and (e), respectively, which exclude the one outlying data point.

Oxygen Isotopic Composition, Temperature, and Salinity of Calcite Precipitation Fluid

The relationship between calcite contents with $\delta^{18}O$ is shown on Figs. 2c and 2d. Obviously, these samples exhibit a strong inverse correlation between these two parameters because calcite cements are enriched in ^{16}O compared to their host dolomite. Due to the temperature dependence of oxygen isotope fractionation during calcite precipitation, it can be inferred that the calcite precipitated under higher temperature than of their enclosing dolomites. By calculating using Figs. 2c and 2d, as previously discussed, the $\delta^{18}O$ values of the calcite cements would be -8.66‰ and -11.04‰, respectively. In Fig. 4b, these $\delta^{18}O$ values in conjunction with homogenization temperature of fluid inclusions of these samples (Fig. 4a) used to exhibit the calcite precipitating fluid had oxygen isotopic composition of +5‰ to +13‰. In contrast to the -1‰ to -5‰ SMOW $\delta^{18}O$ values of Triassic seawater, the calcite would be precipitated from high salinity fluid.

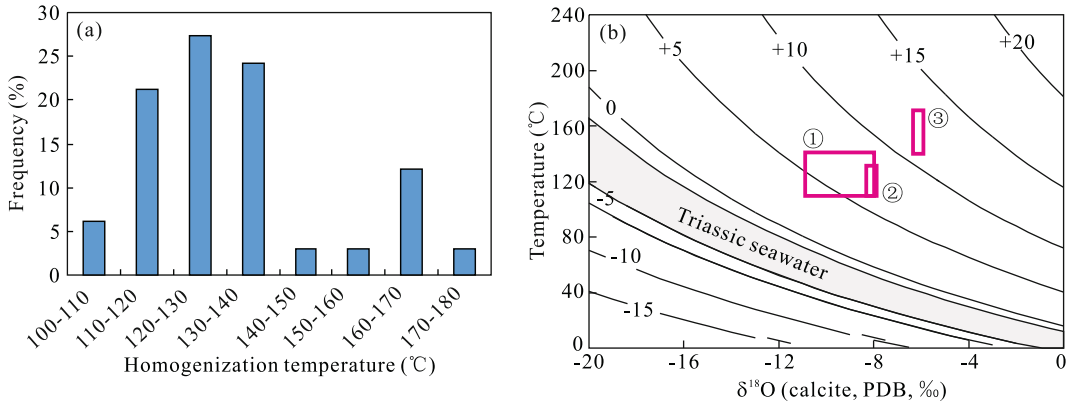

Figure 4. (a) Distribution of homogenization temperature from primary fluid inclusions in Jialingjiang Formation calcite cements of Triassic dolomites, Well HB-1, NE Sichuan basin; (b) equilibrium relationship between $\delta^{18}O$ of calcite, $\delta^{18}O$ of water, and fluid inclusion homogenization temperature (T_h); contours are for oxygen isotopic composition of water equilibriumed with the calcite, and the pattern is taken from Huang (2010); the $\delta^{18}O$ values of Triassic seawater are from Veizer et al. (1999); the range of $\delta^{18}O$ medium values of atmospheric water is from 15 contemporary meteoric water samples, which were taken from Pacific Ocean, as Ren et al. (2000) reported; the data of square section ① are from pore-filling calcites (Figs. 2a–2c), which were developed in silty to finely crystalline dolomite, as listed in Table 1; the data of square section ② are from Huang et al. (2007a); the data of square section ③ are from Wang et al. (2007).

Strontium, Manganese, and Ferrous Contents and CL Features

As previously discussed, continued TSR process should produce a progressively higher Sr^{2+} in the pore waters, resulting in an increased incorporation of strontium in calcite. The silty to finely crystalline dolomite in Member 2 of Jialingjiang Formation show a positive correlation between the calcite fraction and the strontium concentration (Figs. 3e and 3f). This can be interpreted to indicate that the calcite cements are enriched in strontium relative to dolomite matrix. Using the calculation discussed in the previous section, the strontium content of the sample would be 1 573.69×10^{-6} from curve in Fig. 3e and 1 431.58×10^{-6} from curve in Fig. 3f. The result indicates that the pore-filling calcites (Figs. 2a–2c) of Jialingjiang Formation are precipitated from a fluid with high strontium content (Fig. 3b).

Manganese and iron concentrations have also been measured and plotted versus calcite fractions. However, the absence of correlation between them (Fig. 5) indicates that Mn and Fe concentrations are not the sensitive indicators of TSR. In addition, the manganese contents of all samples are less (Table 1), which range from 12×10^{-6} to 71×10^{-6}, with an average of 31×10^{-6} (Table 1). These samples, of course, commonly exhibit very dull luminescence during CL examination (manganese as an activator for luminescence). All the samples also have very low Mn/Sr ratios (ranging from 0.004 to 0.56 with an average of

0.22; see Table 1) and Mn/Sr <2 is a typical signature of carbonates unaltered by meteoric fluids (Huang, 2010, 2008b; Kaufman et al., 1993, 1992). Therefore, the geochemical data of these samples would generally represent the original information of seawater. The concentrations of iron might be complicated because it has a wide variety of sources and sinks such as the clay minerals and other iron-rich aluminosilicates. However, the total iron contents of these diagenetically altered dolomites are primarily less than 1 000 ppm (Fig. 5b), which are slightly depleted compared to most other dolomites. All these trace elemental information for the dolomite samples maybe mostly relevant to seawater. Therefore, seawater (more exactly, the changed seawater) was the principal agent of dolomitization fluids and calcite precipitation fluids.

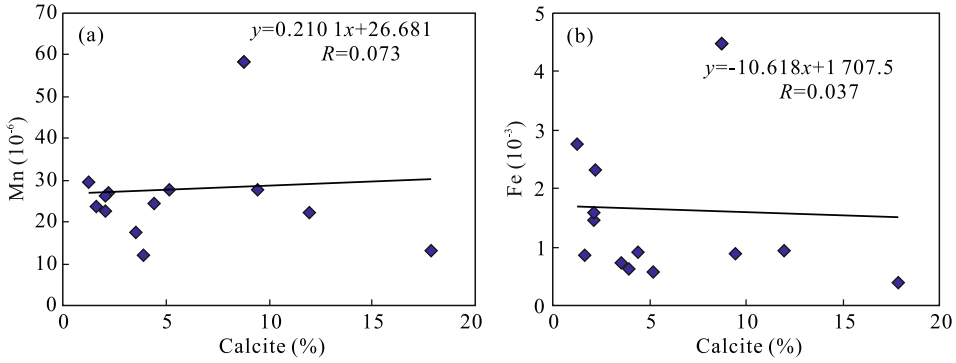

Figure 5. Crossplots of Mn and Fe concentration vs. TSR calcite concentration.

CONCLUSIONS

TSR is widespread in the Triassic deposits, NE Sichuan basin. Authigenic calcites occur as blocky calcite spar cements in fill of primary porosity and are found predominantly in Triassic dolomites, especially the dolomites with evaporates.

The high negative $\delta^{13}C$ values, the high homogenization temperatures, and the high strontium content are the most important features indicative of TSR origin for calcite cements in Triassic, NE Sichuan basin, which can be used to distinguish the authigenic calcites produced by TSR.

The formation of the calcites, developed primarily in silty to finely crystalline dolomites, is controlled primarily by TSR rather than dedolomitization.

The TSR calcites have precipitated from solution with high salinity (water salinities more than that of marine water), low manganese content, and low Mn/Sr ratios. Therefore, under CL, they display very dull luminescence. It suggests that the TSR calcites precipitation fluids should be relevant to marine originated water.

Although tremendous quantities of H_2S and CO_2, which may have enhanced impact on the reservoir quality, could be produced, TSR would reduce porosity and permeability due to extensive calcite cements.

REFERENCES CITED

Broglio Loriga, C. B., Neri, C., Posenato, R., 1986. The Werfen Formation (Lower Triassic) in the Costabella Mt., Uomo Section. In: Italian IGCP 203 Group, ed., Field Guide-Book: Field Conference on Permian and Permian–Triassic Boundary in the South-Alpine Segment of the Western Tethys. Società Geologica Italiana, Brescia. 116–133

Cai, C. F., Xie, Z. Y., Worden, R. H., et al., 2004. Methane-Dominated Thermochemical Sulphate Reduction in the Triassic Feixianguan Formation in East Sichuan Basin, China: Towards Prediction of Fatal H_2S Concentrations. *Marine and Petroleum Geology*, 21: 1265–1279, doi:10.1016/j.marpetgeo.2004.09.003

Horacek, M., Brandner, R., Abart, R., 2007. Carbon Isotope Record of the P/T Boundary and the Lower Triassic in the Southern Alps: Evidence for Rapid Changes in Storage of Organic Carbon. *Palaeogeography, Palaeoclimatology, Palaeoecology*, 252: 347–354, doi:10.1016/j.palaeo.2006.11.049

Huang, S. J., 2010. Carbonate Diagenesis. Geological Publishing House, Beijing (in Chinese)

Huang, S. J., Qing, H. R., Hu, Z. W., et al., 2007a.

Closed-System Dolomitization and the Significance for Petroleum and Economic Geology: An Example from Feixianguan Carbonates, Triassic, NE Sichuan Basin of China. *Acta Petrologica Sinica*, 23(11): 2955–2962 (in Chinese with English Abstract)

Huang, S. J., Qing, H. R., Hu, Z. W., et al., 2007b. Influence of Sulfate Reduction on Diagenesis of Feixianguan Carbonate in Triassic, NE Sichuan Basin of China. *Acta Sedimentologica Sinica*, 25(6): 815–824 (in Chinese with English Abstract)

Huang, S. J., Qing, H. R., Huang, P. P., et al., 2008a. Evolution of Strontium Isotopic Composition of Seawater from Late Permian to Early Triassic Based on Study of Marine Carbonates, Zhongliang Mountain, Chongqing, China. *Science in China* (*Ser. D*), 51(4): 528–539, doi:10.1007/s11430-008-0034-3

Huang, S. J., Wang, C. M., Huang, P. P., et al., 2008b. Scientific Research Frontiers and Considerable Questions of Carbonate Diagenesis. *Journal of Chengdu University of Technology* (*Natural Science*), 35(1): 1–10 (in Chinese with English Abstract)

Kaufman, A. J., Jacobsen, S. B., Knoll, A. H., 1993. The Vendian Record of Sr- and C-Isotope Variations in Seawater: Implications for Tectonics and Paleoclimate. *Earth Planet Sci. Lett.*, 120: 409–430, doi:10.1016/0012-821X(93)90254-7

Kaufman, A. J., Knoll, A. H., Awramik, S. M., 1992. Biostratigraphic and Chemostratigraphic Correlation of Neoproterozoic Sedimentary Successions: Upper Tindir Group, Northwestern Canada, as a Test Case. *Geology*, 20: 181–185, doi:10.1130/0091-7613(1992)020<0181:BACCON>2.3.CO;2

Korte, C., Kozur, H. W., Bruckschen, P., et al., 2003. Strontium Isotope Evolution of Late Permian and Triassic Seawater. *Geochimica et Cosmochimica Acta*, 67(1): 47–62, doi:10.1016/S0016-7037(02)01035-9

Lepper, J., Röhling, H. G., 1998. Buntsandstein. *Hallesches Jb. Geowiss., B*, 6: 27–34

Ma, Y. S., Guo, T. L., Zhao, X. F., et al., 2008. The Formation Mechanism of High-Quality Dolomite Reservoir in the Deep of Puguang Gas Field. *Science in China* (*Ser. D*), 51(Suppl. II): 53–64, doi:10.1007/s11430-008-5020-2

Ma, Y. S., Guo, T. L., Zhu, G. Y., et al., 2007. Simulated Experiment Evidences of the Corrosion and Reform Actions of H_2S to Carbonate Reservoirs: An Example of Feixianguan Formation, East Sichuan. *Chinese Science Bulletin*, 52(Suppl. 1): 178–183, doi: 10.1007/s11434-007-6019-3

Machel, H. G., 2001. Bacterial and Thermochemical Sulfate Reduction in Diagenetic Settings—Old and New Insights. *Sedimentary Geology*, 140: 143–175, doi:10.1016/S0037-0738(00)00176-7

McKee, E., 1954. Stratigraphy and History of the Moenkopi Formation of Triassic Age. *The Geologic Society of America Memoir*, 61: 1–133

Payne, J. L., Lehrmann, D. J., Wei, J. Y., et al., 2004. Large Perturbations of the Carbon Cycle during Recovery from the End-Permian Extinction. *Science*, 305(5683): 506–509, doi:10.1126/science.1097023

Ren, J. G., Huang, Y. P., Fang, Z. S., et al., 2000. Oxygen and Hydrogen Isotope Composition of Meteoric Water in the Tropical West Pacific Ocean. *Acta Oceanologica Sinica*, 22(5): 60–64 (in Chinese with English Abstract)

Veizer, J., Ala, D., Azmy, K., et al., 1999. $^{87}Sr/^{86}Sr$, $\delta^{13}C$ and $\delta^{18}O$ Evolution of Phanerozoic Seawater. *Chemical Geology*, 161: 59–88, doi:10.1016/S0009-2541(99)00081-9

Wang, Y. G., Wen, Y. C., Hong, H. T., et al., 2007. Diagenesis of Triassic Feixianguan Formation in Sichuan Basin, Southwest China. *Acta Sedimentologica Sinica*, 25(6): 831–839 (in Chinese with English Abstract)

Worden, R. H., Smalley, P. C., 1996. H_2S-Producing Reactions in Deep Carbonate Gas Reservoirs: Khuff Formation, Abu Dhabi. *Chemical Geology*, 133: 157–171, doi:10.1016/S0009-2541(96)00074-5

Zhu, G. Y., Zhang, S. C., Liang, Y. B., et al., 2005. Isotopic Evidence of TSR Origin for Natural Gas Bearing High H_2S Contents within the Feixianguan Formation of the Northeastern Sichuan Basin, Southwestern China. *Science in China* (*Ser. D*), 48(11): 1960–1971, doi:10.1360/082004- 147

Zhu, G. Y., Zhang, S. C., Liang, Y. B., et al., 2006a. Dissolution and Alteration of the Deep Carbonate Reservoirs by TSR: An Important Type of Deep-Buried High-Quality Carbonate Reservoirs in Sichuan Basin. *Acta Petrologica Sinica*, 22(8): 2182–2194 (in Chinese with English Abstract)

Zhu, G. Y., Zhang, S. C., Liang, Y. B., et al., 2006b. Characteristics of Gas Reservoirs with High Content of H_2S in the Northeastern Sichuan Basin and the Consumption of Hydrocarbons due to TSR. *Acta Sedimentologica Sinica*, 24(2): 300–308 (in Chinese with English Abstract)